Application of CoFe$_2$O$_4$@CuS magnetic nanocomposite as a novel adsorbent for removal of Penicillin G from aqueous solutions: Isotherm, kinetic and thermodynamic study

Mohammad Kamranifar[a], Ali Allahresani[b], Ali Naghizadeh[a],*

[a]*Medical Toxicology and Drug Abuse Research Center (MTDRC), Birjand University of Medical Sciences, Birjand, Iran, email: mo.kamrani@yahoo.com (M. Kamranifar), Tel. +985632395441, Fax +985632381665, email: al.naghizadeh@yahoo.com (A. Naghizadeh)*
[b]*Department of Chemistry, Faculty of Science, University of Birjand, Birjand, Iran, email: a_allahresani@birjand.ac.ir (A. Allahresani)*

ABSTRACT

In this study, CoFe$_2$O$_4$@CuS magnetic nanocomposite was synthesized and used to removal of Penicillin G (PG) from aqueous solutions. The synthesized magnetic nanocomposite were characterized with scanning electron microscopy (SEM), transmission electron microscopy (TEM), fourier transform infrared spectroscopy (FTIR), X-ray diffraction (XRD), vibrating-sample magnetometer (VSM).Also, the impact of major parameters including pH (3–11), adsorbent dosage (0.2–0.8 g/L), PG concentration (10–100 mg/L), contact time (10–120 min) and temperature (283–313 K) were studied. Finally, isotherm, kinetic and thermodynamics of adsorption process of PG onto CoFe$_2$O$_4$@CuS magnetic nanocomposite were investigated. According to the results of this study, CoFe$_2$O$_4$@CuS magnetic nanocomposite used to adsorption of PG in optimum condition has maximum adsorption capacity of 41 mg/g (optimum condition pH = 5, adsorbent dosage: 0.2 g/L, PG concentration: 100 mg/L, contact time: 40 min and temperature 313 K). Results of thermodynamic study showed that all the values of ΔG, ΔH and ΔS were positive. Also isotherm study showed that adsorption of PG on CoFe$_2$O$_4$@CuS magnetic nanocomposite better compatibility with Langmuir and then Temkin, Freudlich and Dubinin-Radushkevich models. Also, by comparing the kinetics of the adsorption process, it was determined that the pseudo-second order kinetics was able to provide a better description of the kinetics of adsorption.

Keywords: Magnetic nanocomposite; Penicillin G; Isotherm; Kinetic; Thermodynamic

1. Introduction:

Nowadays, overuse of antibiotics and the entrance of them into the aquatic environment have caused many problems [1]. Annually, about 0.1–0.2 million tons of antibiotics are used around the world [1–3]. In addition to medicine, the use of antibiotics in agriculture has increased [4]. In animal husbandry, antibiotics as growth promoters are primarily added to the animals feed [5]. Furthermore, antibiotics are used to treat infections in farm animals [6].

β-lactam antibiotics are great groups of antibiotics with aβ-lactam ring in their chemical structures [7]. These antibiotics include penicillins, cephalosporins and related compounds [7]. These factors are active against many gram positive, gram negative and anaerobic organisms. β-lactam antibiotics affect on the cell wall of the bacteria by interfering with the structure of peptidoglycans [7]. Penicillins are the first group of β-lactam antibiotics. Penicillins act on the synthesis of peptidoglycans and cause cell lysis and organisms death [8,9]. Meanwhile, Penicillin G (PG) is the most active molecule that has been developed more than half a century and used for patient treatment [9]. The chemical structure of PG with molecular formula of C$_{16}$H$_{17}$KN$_2$O$_4$S and molecular weight of 372.48 g/mol is shown in Fig. 1.
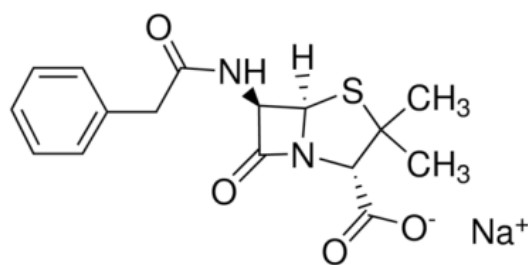
*Corresponding author.

Fig. 1. Chemical structure of PG [10].

Antibiotics are not metabolized completely after ingestion, and 30–90% of them remain active after excretion [11]. Antibiotics have a different half-life in the environment, some of them are very stable and therefore their level of contamination increases in the environment [12]. The introduction of pharmaceutical compounds into the environment can lead to serious problems for human health and terrestrial organisms [13,14]. Antibiotics are suspected of producing resistant microorganisms which cause serious health problems [15,16]. Moreover, antibiotics can remain in the environment for a long time because of high stability, lipophilic and low biodegradability that this causes the compounds to be dangerous even at low concentrations [17,18]. Therefore, antibiotics should be removed prior to entering the recipient water.

In recent years, various studies have been done to reduce these pollutants (antibiotics) from aquatic environments. Meanwhile, some processes such as reverse osmosis [19], photocatalytic degradation [20,21], photo Fenton [22], coagulation [23], ion exchange [24] and surface adsorption [25] can be mentioned. However, some of these methods have various disadvantages including low efficiency, high costs and production of toxic byproducts that limit these methods [26]. Among these methods, adsorption is one of the most widely used for removal of various pollutants [13]. Adsorption is a simple method compared to other methods, and has a low sensitivity to the flow fluctuations and has high flexibility and low operating cost which is applicable for separation of contaminants from aqueous environments. Therefore, many researchers have focused on optimizing the adsorption process and finding new adsorbents with high adsorption capacity and low costs [27,28]. Among various adsorbents, activated carbon is the most common adsorbent used in water and wastewater treatment. But, this adsorbent has disadvantages such as high costs and the need for frequent resuscitation [29]. In recent years, much attention has been paid to nanotechnology in the treatment of water and wastewater [30,31]. Nanoparticles can be used to removal of pollutants due to their small size, large specific surface areas and high mobility [31]. Meanwhile, magnetic nanoparticles can be a proper adsorbent for removal of contaminants due to various properties such as high surface area and easy separation under magnetic fields [32]. In recent years, many efforts have been made to prepare and synthesize of magnetic nanoparticles to apply them in a variety of fields. In general, the performance and application of these nanoparticles are influenced by their design and synthesis. Until now, various magnetic nanoparticles, such as pure metal nanoparticles (Fe, Co, Ni), metal oxides (Fe_3O_4, γ-Fe_2O_3), ferrites (MFe_2O_4, M = Cu, Ni, Mn, Mg, etc), metal alloys (FePt, CoPt) have been synthesized [33]. Among them, cobalt ferrite magnetic nanoparticles with spinel structure have a significant chemical stability and have been used in various fields [34].

In this study, $CoFe_2O_4$@CuS magnetic nanocomposite was used to removal of PG from aqueous solutions and parameters including pH, adsorbent dosage, contact time, PG concentration, temperature and thermodynamic of process were investigated. Finally, Isotherm and kinetic of the adsorption process were studied.

2. Material and methods

2.1. Synthesis of $CoFe_2O_4$ magnetic nanoparticles

$Fe(NO_3)_3 \cdot 9H_2O$ and $Co(NO_3)_2 \cdot 6H_2O$ were used to synthesize cobalt ferrite nanoparticles. First, ($Fe(NO_3)_3 \cdot 9H_2O$ as well as $Co(NO_3)_2 \cdot 6H_2O$) were dissolved separately in deionized water and then added to each other. Thereafter, 1 M solution of NaOH was added to the solution and it was stirred at 80°C for 2 h. After the formation of cobalt ferrite nanoparticles, these nanoparticles were separated by an external magnet and finally washed with deionized water and ethanol [35].

2.2. Synthesis of $CoFe_2O_4$@CuS magnetic nanocomposite

$CuSO_4$ was used to modify the surface of cobalt ferrite nanoparticles. First, a certain amount of cobalt ferrite nanoparticles (0.15 g) was dispersed in an ethylene glycol solvent and then $CuSO_4$ added to this solution at 120°C. After dissolving $CuSO_4$, $Na_2S_2O_3$ solution (previously made by dissolving it in ethylene glycol) was added to $CuSO_4$ solution and the reaction mixture was refluxed at 140°C for 90 min. The resultant nanocomposite was separated by magnet and washed several times with deionized water and ethanol and finally dried in a vacuum oven for 5 h [36].

2.3. Characteristics of $CoFe_2O_4$@CuS magnetic nanocomposite

In this study, FTIR, XRD, SEM, TEM and VSM analyses were used to determine the structural properties of $CoFe_2O_4$ magnetic nanoparticles and $CoFe_2O_4$@CuS magnetic nanocomposite.

2.4. Determination of pH_{zpc}

For determination of pH_{zpc}, 0.25 g of $CoFe_2O_4$@CuS magnetic nanocomposite was added to erlenmeyer flasks containing 50 mL of distilled water, which the pH had already been adjusted between 2–12 and it was placed on the shaker. After passing 24 h, samples were taken from shaker and their pHs were determined again.

2.5. Adsorption experiments

In this research, the experiments were performed in batch system. All chemicals purchased from Merck

Company. PG provided from Sigma Aldrich and used to prepare the stock solution (500 mg/L). Other concentrations of PG were made by dilution of the stock solution. Then, the effect of different parameters on removal of PG by $CoFe_2O_4@CuS$ magnetic nanocomposite such as pH (3–11), adsorbent dosage (0.2–0.8 g/L), PG concentration (10–100 mg/L), contact time (10–120 min) and temperature (283–313 K) were studied. 1 and 0.1 N solution of HCl and NaOH were used to adjust the pH (pH meter Hach, HQ411d, USA). Shaker (Multi shaker, NB-101MT, Korea) was used to mixing the sample. Also, Incubator shaker (Incubator shaker, SI-100R, Korea) was used to adjust the temperature of solutions. Finally, after separating the nanoparticle by the external magnet and passing through 0.45 micron filter and centrifugation, PG concentration was determined by a UV-visible spectrophotometer (UV/Vis Spectrophotometer T80+, PG Instrument) at a wavelength of 290 nm [37]. Then, the adsorption capacity, isotherms, kinetics and thermodynamics of the PG adsorption process on the $CoFe_2O_4@CuS$ magnetic nanocomposite were obtained using the formulas in Table 1 [38–41].

3. Results and discussion

3.1. Characteristics of adsorbent

3.1.1. FT-IR analysis

Fig. 2A shows FT-IR spectrum of $CoFe_2O_4$ magnetic nanoparticles. The vibration peak observed in 3406 cm^{-1} is related to the O-H group. Also, the vibration peak of 410 cm^{-1} and 600 cm^{-1} are related to the Co-O and Fe-O, responsibility [42,43]. Fig. 2B shows FT-IR spectrum of $CoFe_2O_4@$ CuS magnetic nanocomposite. In this spectrum, the vibration peak observed in 3227 cm^{-1} refers to the O-H group. In addition, the vibration peaks of 669 cm^{-1}, 412 cm^{-1}, and 583 cm^{-1} are Cu-O, Co-O and Fe-O groups, respectively [42–44].

3.1.2. XRD analysis

Fig. 3A shows XRD analysis of $CoFe_2O_4$ magnetic nanoparticles. The relative positions and relative intensity of all peaks represent the formation of $CoFe_2O_4$ magnetic nanoparticles with a crystalline structure and a cubic spinel, which is very close to the values of the literature with

Table 1
The isotherms, kinetic, and thermodynamic equations used for adsorption of PG onto $CoFe_2O_4@CuS$

Adsorption capacity	Isotherm equations	Kinetic equations	Thermodynamic equations
Adsorption capacity $$q_e = \frac{C_o - C_e}{m}V$$	Langmuir model $$q_e = \frac{Q_m K_L C_e}{1 + K_L C_e}$$	Pseudo-first-order $$\frac{dq_t}{dt} = K_1(q_e - q_t)$$	Van' t Hoff $$\Delta G° = -RT\ln kd$$
	Equilibrium parameter (R_L) $$R_L = \frac{1}{(1 + bC_0)}$$	Pseudo-second-order $$\frac{dq_t}{dt} = K_2(q_e - q_t)^2$$	Free energy of adsorption $$\mathrm{Ln}k_d = -\frac{\Delta H°}{RT} + \frac{\Delta S°}{R}$$
	Freundlich model $$q_e = K_f C_e^{\frac{1}{n}}$$		
	BET model $$Q_e = \frac{q_{\max} K_b C_e}{(C_s - C_e)\left(1 + (K_b - 1)\left(\frac{C_e}{C_s}\right)\right)}$$		
	Temkin model $$q_e = \frac{RT}{b_T}\ln(A_T C_e)$$		
	Dubinin-Radushkevich $$q_m = e^{-\beta \varepsilon^2} q_e$$		
	Polanyi potential $$\varepsilon = RT\ln\left(1 + \left(\frac{1}{C_e}\right)\right)$$		

q_e (mg/g), C_o (mg/L), C_e (mg/L), m (g), V (L), Q_m (mg/g), K_L (L/mg), q_{max} (mg/g), C_s is (mg/L), b_T (J/mol), A_T (L/g), β (mol^2/kj^2), ε (J/mol), K_1 (1/min), K_2 (g/mg·min), q_t (mg/g), R (8.314 J/mol·K), $\Delta H°$ (kj/mol), $\Delta S°$ (J/mol·K), T (K)

(A)

(B)

Fig. 2. FTIR spectrum (A) $CoFe_2O_4$ (B) $CoFe_2O_4$@CuS.

(A)

(B)
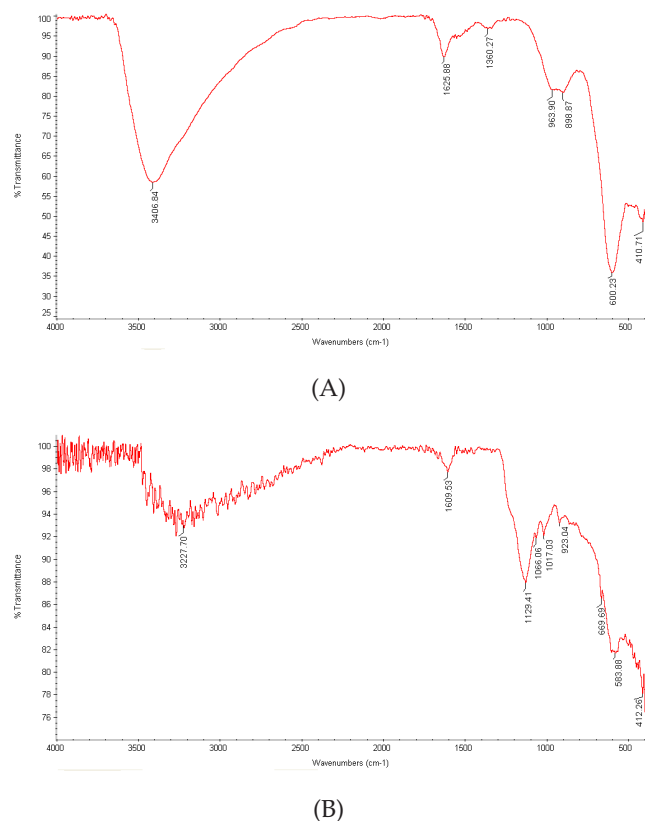
Fig. 3. XRD pattern (A) $CoFe_2O_4$ (B) $CoFe_2O_4$@CuS.

the JCPDS number (JCPDS No. 01-1121). In this pattern, the 2Θ of 18.4, 30.3, 35.6, 35.3, 43.3, 53.6, 57.1 and 62.8 are related to Miller's indexes 611, 220, 311, 400, 422 , 511 and 440, respectively [35,45]. Fig. 3B shows XRD spectrum of $CoFe_2O_4$@CuS magnetic nanocomposite. The XRD pattern of $CoFe_2O_4$@CuS magnetic nanocomposite showed some changes to the XRD pattern of $CoFe_2O_4$ magnetic nanoparticle. New 2Θ can be related to CuS, which is in accordance with the JCPDS number (JCPDS No. 65-3556) [36]. In these XRD pattern, the sharp peaks indicate its highly crystalline state. Also, the average crystallite size of the nanoparticles was determined using an intense peak of XRD pattern. For this purpose, the Debye-Scherrer formula was used:

$$D = \frac{K\lambda}{\beta\cos\varnothing} \qquad (1)$$

where D is particle size, k is constant, λ for Cu is 1.54Å, β is the peak width of the diffraction peak profile at half maximum height resulting from small crystallite size (FWHM) and θ is the corresponding angle of diffraction [46]. The calculated results showed that the size of the $CoFe_2O_4$ and $CoFe_2O_4$@CuS were 11 and 23 nm, respectively.

3.1.3. SEM analysis

Figs. 4A,B show SEM images of the $CoFe_2O_4$ nanoparticles and $CoFe_2O_4$@CuS magnetic nanocomposite, responsibility. These images show that the synthesized nanoparticles are almost spherical [14,36]. Also, size of the nanoparticles
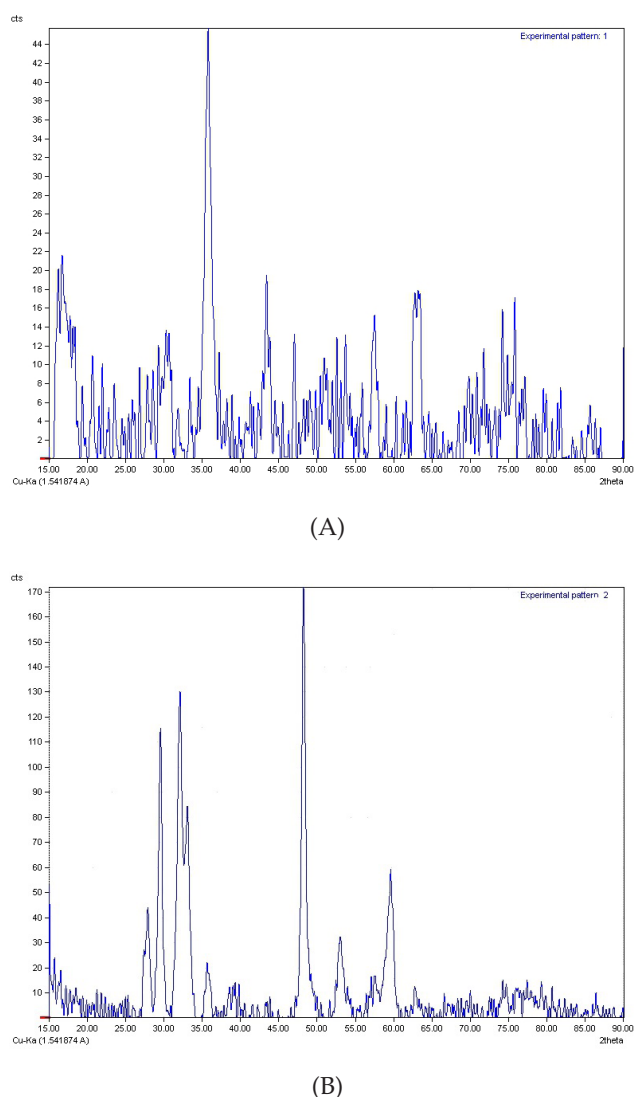
($CoFe_2O_4$ and $CoFe_2O_4$@CuS) was less than 100 nm. In these images, the accumulation of nanoparticles is evident.

3.1.4. TEM analysis

TEM images of $CoFe_2O_4$ magnetic nanoparticles and $CoFe_2O_4$@CuS magnetic nanocomposite are shown in Fig. 5A and 5B, respectively. Generally, the size of nanoparticles was less than 100 nm and the images confirm this. Also, in Fig. 5B, it is clear that the size of $CoFe_2O_4$ magnetic nanoparticles by modifying with CuS has grown, and CuS particles are coated on $CoFe_2O_4$. The TEM image (Fig. 5B) shows a core-shell structure of the nanoparticles, although a large amount of aggregation has been observed.

3.1.5. VSM analysis

VSM analysis was used to investigate the magnetic property of $CoFe_2O_4$ magnetic nanoparticle and $CoFe_2O_4$@
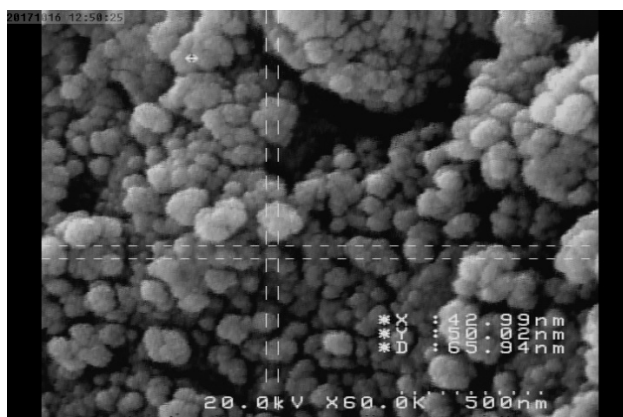
(A)

(B)

Fig. 4. SEM image (A) $CoFe_2O_4$ (B) $CoFe_2O_4$@CuS.

(A)

(B)
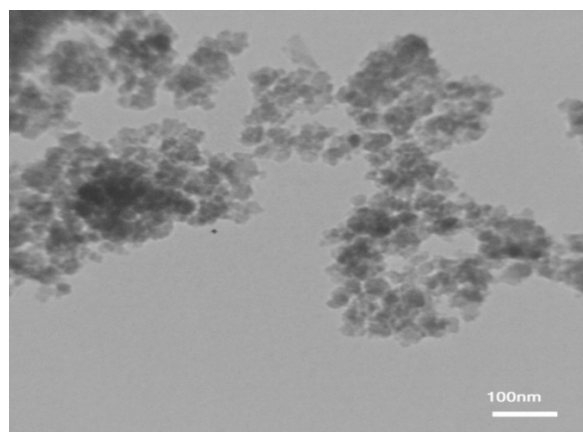
Fig. 5. TEM image (A) $CoFe_2O_4$ (B) $CoFe_2O_4$@CuS.

CuS magnetic nanocomposite. The magnetic hysteresis loops in Figs. 6A,B show that these nanoparticles respond to an external magnetic. A saturation magnetization of 42.04 emu/g is obtained on the $CoFe_2O_4$ magnetic nanoparticles which decreases to 7.76 emu/g due to the modification process and synthesized the $CoFe_2O_4$@CuS magnetic nanocomposite. However, the magnetic properties of the nanoparticles are reduced, but they have a sufficient magnetic response for magnetic separation.
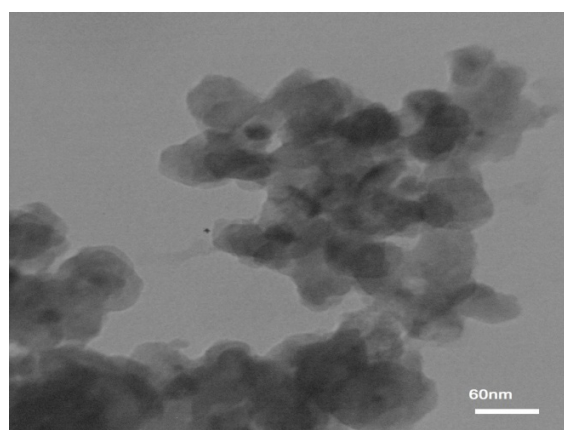
3.2. pH_{zpc} determination

At this stage, as previously noted, a certain amount of nanoparticles was added to Erlenmeyer flasks containing distilled water, which pH had already been adjusted between 2–12 and it was placed on the shaker. After passing 24 h pHs were read again. Fig. 7 shows the results of this stage. As shown, pH_{zpc} for nanoparticles used in this study is about 5.2.

3.3. Effect of pH

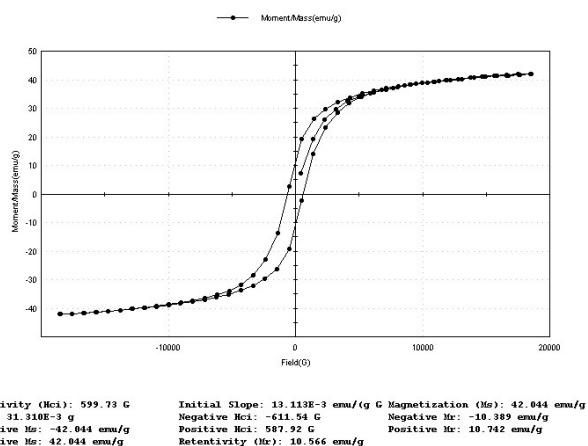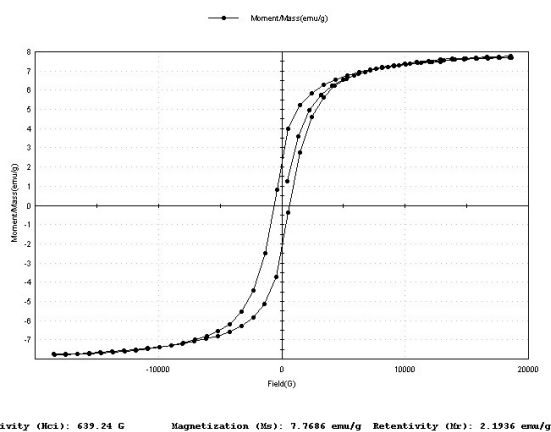To determine the optimal pH, a PG solution was made at a concentration of 30 mg/L and the variable range of pH was adjusted between 3–11. Then, 0.2 g/L of adsorbent was added to the solution and was placed on the shaker for 60 min. As seen in Fig. 8, the highest removal rate of PG is achieved in pH = 5 and after that removal was decreased. In pH = 5 that the highest adsorption capacity occurred (23 mg/g).

The pH of solution has a great influence on the efficiency of adsorption process because pH variations of solution cause change in the surface charge and functional groups chemistry of adsorbent [47]. As results show that highest removal rate of PG by $CoFe_2O_4$@CuS magnetic nanocomposite occurs in pH = 5 (Fig. 8). This is due to the pH_{zpc} of adsorbent and the surface charge of PG. According to Fig. 7, the amount of pH_{zpc} was 5.2. In values higher and lower than pH_{zpc} value, adsorbent surface is occupied by ion OH^- and H^+, respectively which causes adsorbent surface in pHs greater than 5.2 has negative charge but has positive charge in pHs lesser than 5.3 [47,48]. On the other hand, PG is water-soluble and is classified as a weak acid (pKa = 2.75) [49]. In pHs greater than pKa, PG becomes in the form of anion. Therefore, in pHs greater than 5.2 considering negative adsorption surface charge and anionic nature of PG in this pH, The electrostatic repulsive force occurs between the adsorbent and the contaminant that

Coercivity (Hci): 599.73 G   Initial Slope: 13.113E-3 emu/(g G   Magnetization (Ms): 42.044 emu/g
Mass: 31.310E-3 g   Negative Hci: -611.54 G   Negative Mr: -10.389 emu/g
Negative Ms: -42.044 emu/g   Positive Hci: 587.92 G   Positive Mr: 10.742 emu/g
Positive Ms: 42.044 emu/g   Retentivity (Mr): 10.566 emu/g

(A)

Coercivity (Hci): 639.24 G   Magnetization (Ms): 7.7686 emu/g   Retentivity (Mr): 2.1936 emu/g
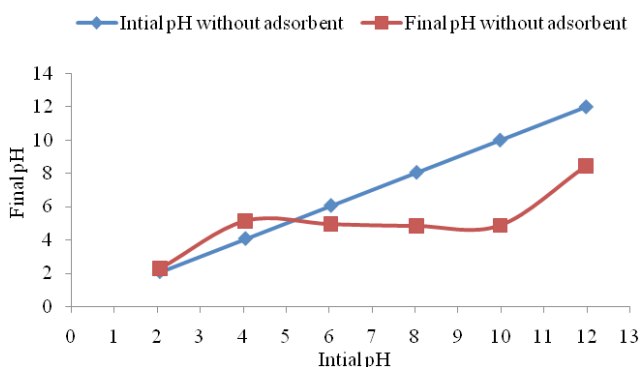
(B)

Fig. 6. VSM analysis (A) $CoFe_2O_4$ (B) $CoFe_2O_4$@CuS.

Fig. 7. pH_{zpc} of $CoFe_2O_4$@CuS.

consequently adsorption amount of PG decreases. Aksu et al, the effect of biosorbent of Rhizospusarrhizus on penicillin G removal was investigated and optimum pH = 6 was obtained [50]. These authors stated that biosorbent surface (Rhizospusarrhizus) had a negative charge at pHs higher than 2.5 and 3.5. Penicillin G anions in the pH = 6 do not interact electrostatically with adsorbent (negative
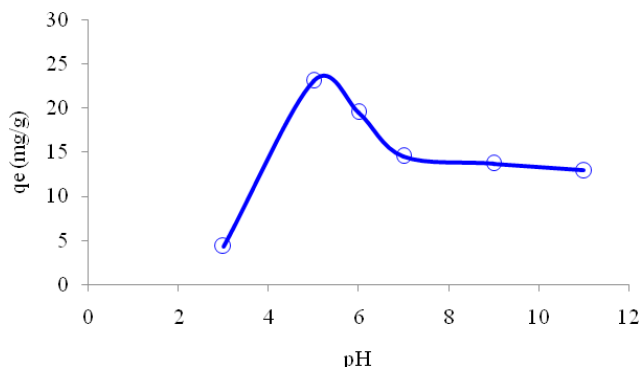

Fig. 8. Effect of pH for the adsorption of PG onto $CoFe_2O_4$@CuS (PG concentration: 30 mg/L, adsorbent dosage: 0.2 g/L, contact time: 60 min).

charge surface). These anions are probably adsorbed by physical or chemical forces [50].

3.4. Effect of adsorbent dosage

In this stage to determine optimum adsorbent dosage, values of 0.2–0.8 g/L of $CoFe_2O_4$@CuS magnetic nanocomposite were added to PG solution with concentration of 30 mg/L in pH = 5. According to the results, maximum adsorption capacity was showed in adsorbent dosage of 0.2 g/L (Fig. 9). By increasing the adsorbent dosage from 0.2 g/L to 0.8 g/L, the adsorption capacity decreased from 23 to 7 mg/g.

As adsorbent value increases, accessible and exchangeable sites of nanoparticles increase which this leads to increase the removal of contaminant [51]. But in other hand, due to increase adsorbent dosage, active adsorbent sites are much more than saturated threshold adsorption points. Therefore, only part of the active adsorbent sites has been occupied by the PG molecules that lead to decrease of adsorption capacity [52]. In this regard, similar results were obtained by Balarak et al. on removal of PG by Lemna minor [53]. The researchers for the reason of subject said that the reduction of the Lemna minor adsorption capacity can be due to two reasons. First, the particles of adsorbent accumulate with increasing adsorbent dose, and hence the surface of the total adsorbent is reduced. Secondly, by increasing the adsorbent dose, active adsorbent sites were not completely saturated [53].

3.5. Effect of PG concentration and contact time

In the stage of the effect of PG concentration and contact time, according to the results of previous stages (optimum pH = 5 and adsorbent dosage = 0.2 g/L), after preparing PG solutions with concentrations of 30, 50, 70 and 100 mg/L, 0.2 g/L of adsorbent dosage was added to the solution and shaken for 10–120 min. Fig. 10 shows the results of the study of initial concentration effect of antibiotic and contact time on the removal of PG by $CoFe_2O_4$@CuS magnetic nanocomposite. According to this figure, by increasing the antibiotic concentration, the adsorption capacity increased. The highest adsorption capacity occurred at time = 40 min and then the adsorption capacity has reached equilibrium.
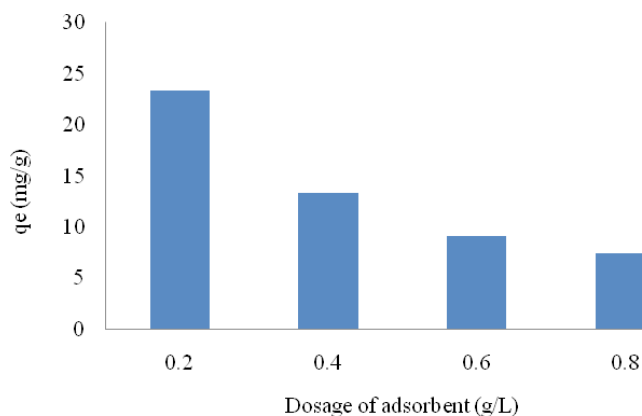
Fig. 9. Effect of adsorbent dosage for the adsorption of PG onto CoFe$_2$O$_4$@CuS (PG concentration: 30 mg/L, pH: 5, contact time 60 min).

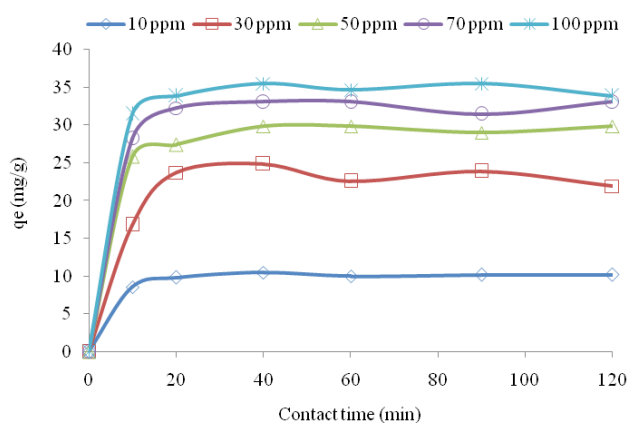

Fig. 10. Effect of PG concentration and contact time for the adsorption of PG onto CoFe$_2$O$_4$@CuS (adsorbent dosage: 0.2 g/L, pH: 5).

As shown in Fig. 10, as the contact time increases, due to the increased opportunity and chance of collision of PG molecules with adsorbent nanoparticles, the amount of adsorption increases. When contact time between adsorbent and solutions containing PG increases, the amount of adsorption increases. High adsorption capacity in initial stage can be due to higher driving force which promotes the rapid transfer of PG molecules to adsorbent surfaces as well as the availability of a large number of active sites in the adsorbent. After that, amount of adsorption decreases gradually and is balanced approximately at 40 min. Reducing the adsorption rate may be due to the reduction of residual active adsorbent sites and the prolonged and slow penetration of PG molecules into adsorbent cavities [54]. In study of Pouretedal et al. on the removal of Penicillin G, it was found that the balance time in this study was 8 h [37].

In addition, the result of this research showed that the adsorption capacity is increased with the increasing of the PG concentration. The reason for increasing the adsorption capacity can be due to the increase of the transmission force to increase the mass transfer rate and also the increased probability of contact between the adsorbent and the adsor-

bate [55,56]. Similar study was conducted on the removal of PG by Lemna minor [53].

3.6. Effect of the temperature and thermodynamic process

To determine the effect of temperature on the removal of PG by CoFe$_2$O$_4$@CuS magnetic nanocomposite, 4 temperatures of 283, 293, 303 and 313 K were selected and adsorption process was done in optimum conditions (pH = 5, adsorbent dosage = 0.2 g/L, PG concentration 100 mg/L and contact time: 40 min). As shown in Fig. 11, by increasing the temperature the adsorption capacity of CoFe$_2$O$_4$@CuS magnetic nanocomposite was increased. Also, Table 2 shows the results achieved from thermodynamic study of the adsorption process. As shown in this table, all values of ΔG, ΔH and ΔS are positive.

Calculated values of adsorption variables of PG by CoFe$_2$O$_4$@CuS magnetic nanocomposite in Table 2 show that ΔG has positive values. This shows the possibility of non-spontaneous adsorption process that corresponds to the results that adsorption capacity increases with increasing temperature [57]. Another parameter of thermodynamic i.e. ΔS has positive value that this indicates that it has increased randomly during the adsorption process [58]. In addition, positive amount of ΔH indicates that the adsorption process is naturally endothermic and the adsorption capacity increases with increasing temperature [59]. Also, values of |ΔS|>|ΔH| and this indicates that the adsorption process is dominated by entropic rather than enthalpy changes [58].

3.7. Determination of adsorption isotherm

Data of adsorption isotherms of PG by CoFe$_2$O$_4$@CuS magnetic nanocomposite has been presented in Table 3. Based on the correlation coefficients listed in this table, it was determined that removal of PG by CoFe$_2$O$_4$@CuS magnetic nanocomposite follows Langmuir isotherm (R^2 = 0.99) and then it follows Temkin (R^2 = 0.98), Dubinin-Radushkevich (R^2 = 0.97) and Freundlich (R^2 = 0.92).

The analysis of isotherm data can be used for design purposes [60]. In fact, adsorption isotherms express how interaction is occurred between adsorbent and adsorbate [61]. Therefore, this parameter plays a very important role in optimizing the use of an adsorbent and determining the capacity of an adsorbent [62]. In Langmuir model, adsorption happens in some homogeneous and special places inside of adsorbent but in Freundlich isotherm, a heterogeneous and non-uniform surface of the heat of adsorption on the surface of the process performs adsorption. Temkin isotherm is dominated by both theories [50]. One of the important indicators in Langmuir isotherm is parameter without R_L dimension which can be used to evaluate the suitability of CoFe$_2$O$_4$@CuS magnetic nanocomposite for PG adsorption. Value of R_L in this experiment is 0.24 that this value is in 0–1 range, it indicates that the adsorption is desirable [63]. 1/n parameter in Freundlich isotherm shows intensity of surface adsorption. The value of 1/n below one shows normal adsorption process, while 1/n more than one shows cooperative adsorption [64,65]. Hence value of 1/n is between 0–1 (1/n = 0.5), adsorption process is desir-
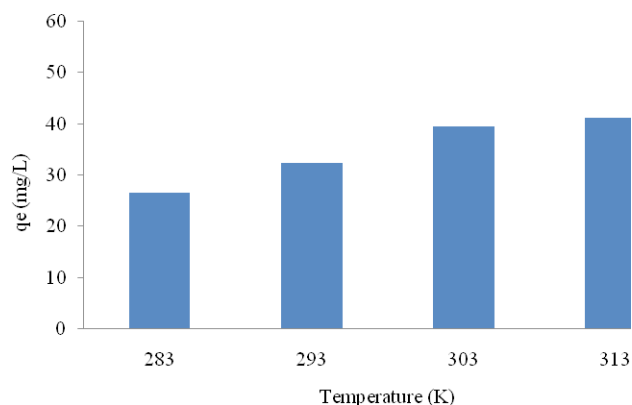
Fig. 11. Effect of temperature for the adsorption of PG onto $CoFe_2O_4$@CuS (pH: 5, adsorbent dosage: 0.2 g/L, PG concentration: 100 mg/L and contact time: 40 min).

Table 2
Thermodynamics parameters of PG adsorption by $CoFe_2O_4$@CuS

T (K)	q_e (mg/g)	Thermodynamics Parameters		
		ΔG (kJ/mol)	ΔH (kJ/mol)	ΔS (J/mol K)
283	26.61	2.72	12.09	33.31
293	32.26	2.31		
303	39.52	1.83		
313	41.13	1.78		

Table 3
Isotherms constants calculations for the adsorption of PG onto $CoFe_2O_4$@CuS

Isotherms	Constants	Values
Langmuir	q_{max} (mg/g)	51.67
	K_L (L/mg)	0.03
	R_L	0.24
	R^2	0.99
Freundlich	k_f (mg/g)	4.33
	$1/n$	0.50
	n	2.00
	R^2	0.92
BET	$1/A \cdot X_m$	0.10
	$(A-1)/(A \cdot X_m)$	0.21
	A	1.02
	X_m	4.97
	R^2	0.02
Temkin	A_T, L/mg	0.41
	b_T	240.68
	B	10.29
	R^2	0.98
Dubinin-Radushkevich	β, mole^2/kJ^2	1E-05
	E, kJ/mole	0.19
	q_m, mg/g	32.43
	R^2	0.97

able [66]. Data of Dubinin-Radushkevich model can be used to determine the nature of adsorption phenomenon. Mean adsorption free energy provides information on the adsorption mechanism. Value of E for $CoFe_2O_4$@CuS magnetic nanocomposite in PG adsorption was 0.19 KJ/mol. If E > 16 kJ/mol, the adsorption process may be subjected to particle diffusion. In addition, if E is between 8–12 KJ/mol, the dominant mechanism of the adsorption process is the type of ion exchange. But for values of E < 8 KJ/mol dominant mechanism of the process is physical [67]. Then, dominant mechanism of adsorption process of PG by $CoFe_2O_4$@CuS magnetic nanocomposite is physical. According to the results from study of Asku et al., adsorption of penicillin by activated carbon follows Langmuir and Redlich Peterson isotherm [50].

3.8. Determination of adsorption kinetics

Results of adsorption kinetics of PG by $CoFe_2O_4$@CuS magnetic nanocompositeis shown in Table 4. By examining the correlation coefficients in these two models, it was determined that the adsorption data follow pseudo second-order kinetic model.

The kinetic evaluation of the adsorption process is important in order to find out the information about factors affecting the reaction speed [62]. In pseudo-first order kinetic, changes in adsorption rate with time are proportional to number of changes in saturated concentration and removal amount of adsorbent with time. In other words,

the reaction rate has a direct relation to the first power of initial concentration. In pseudo-second order model, it is assumed that chemical adsorption is the controller of the adsorption phenomenon and occupancy rate of adsorption sites is proportional to the square of number of unoccupied sites. In other words, reaction rate has a direct relation to the second power of initial concentration [68,69]. By comparing the correlation coefficients between kinetics in Table 3, it can be concluded that the compliance rate of adsorption equilibrium is more than pseudo-second order kinetic that it is similar to the study of Asku et al. [50].

4. Conclusion

Results of the analyses performed in this study (SEM, TEM, FTIR, XRD and VSM) showed that synthesis of $CoFe_2O_4$@CuS magnetic nanocomposite was successful. Results obtained from this study was showed that $CoFe_2O_4$@CuS magnetic nanocomposite to adsorption of PG in optimum condition (pH = 5, nanocomposite dosage: 0.2 g/L, PG concentration: 100 g/L, contact time: 40 min and temperature: 313 K) has maximum adsorption capacity of 41 mg/g. Also, Results of thermodynamic study of adsorption process showed that all values of ΔG, ΔH and ΔS were positive. Study of adsorption isotherm showed that adsorption reaction showed a better match to Langmuir model and then Temkin, Freundlich and Dubinin-Radushkevich. Also,

Table 4
Kinetics constants calculations for the adsorption of PG onto $CoFe_2O_4$@CuS

C_0 (mg/L)	Pseudo-first-order			Pseudo-second-order			q_e exp (mg/g)
	K_1 (min^{-1})	q_e cal (mg/g)	R^2	K_2 (g/mg min)	q_e cal (mg/g)	R^2	
9.8	0.002	1.56	0.04	0.08	10.26	1.00	11.5
27.0	0.004	3.14	0.02	0.09	22.59	0.99	25.8
48.5	0.001	3.36	0.16	0.02	30.02	1.00	30.8
64.1	0.002	2.74	0.06	0.04	32.86	1.00	34.1
96.2	0.002	2.69	0.01	0.16	34.44	1.00	36.5

by comparing the kinetics of the adsorption process, it was determined that the pseudo-second order kinetics was able to provide a better description of the kinetics of adsorption.

Acknowledgment

References

[1] J.L. Martinez, Environmental pollution by antibiotics and by antibiotic resistance determinants, Environ. Pollut., 157 (2009) 2893–2902.

[2] M. Hoseini, G.H. Safari, H. Kamani, J. Jaafari, A. Mahvi, Survey on removal of tetracycline antibiotic from aqueous solutions by nano-sonochemical process and evaluation of the influencing parameters, Iran. J. Health. Environ., 8 (2015) 141–152.

[3] M. Kamranifar, A. Allahresani, A. Naghizadeh, Synthesis and characterizations of a novel $CoFe_2O_4$@CuS magnetic nanocomposite and investigation of its efficiency for photocatalytic degradation of penicillin G antibiotic in simulated wastewater, J. Hazard. Mater., 366 (2019) 545–555.

[4] A. Gulkowska, H.W. Leung, M.K. So, S. Taniyasu, N. Yamashita, L.W. Yeung, B.J. Richardson, A. Lei, J.P. Giesy, P.K. Lam, Removal of antibiotics from wastewater by sewage treatment facilities in Hong Kong and Shenzhen, China, Water. Res., 42 (2008) 395–403.

[5] M. Samadi, R. Shokohi, R. Harati, Comparison of heterogeneous fenton process and adsorption process on magnetic nanocomposite for ciprofloxacin removal from aqueous solutions, J. Qazvin. Univ. Med. Sci., 20 (2016) 4–13.

[6] Q. Xian, L. Hu, H. Chen, Z. Chang, H. Zou, Removal of nutrients and veterinary antibiotics from swine wastewater by a constructed macrophyte floating bed system, J. Environ. Manag., 91 (2010) 2657–2661.

[7] K.B. Holten, Appropriate prescribing of oral beta-lactam antibiotics, Am. Fam. Physician, 62 (2000) 611–620.

[8] A. Bryskier, Antibiotics and antibacterial agents: classifications and structure-activity relationship, in: Antimicrobial Agents, American Society of Microbiology, 2005, pp. 13–38.

[9] A. Bryskier, Penicillins, in: Antimicrobial Agents, American Society of Microbiology, 2005, pp. 113–162.

[10] M. Dehghani, M. Ahmadi, S. Nasseri, Photodegradation of the antibiotic penicillin G in the aqueous solution using UV-A radiation, Iran. J. Health. Sci., 1 (2013) 43–50.

[11] A. Watkinson, E. Murby, S. Costanzo, Removal of antibiotics in conventional and advanced wastewater treatment: implications for environmental discharge and wastewater recycling, Water. Res., 41 (2007) 4164–4176.

[12] M.B. Ahmed, J.L. Zhou, H.H. Ngo, W. Guo, Adsorptive removal of antibiotics from water and wastewater: Progress and challenges, Sci. Total Environ., 532 (2015) 112–126.

[13] V. Homem, L. Santos, Degradation and removal methods of antibiotics from aqueous matrices–a review, J. Environ. Manag., 92 (2011) 2304–2347.

[14] G.H. Safari, M. Hoseini, M. Seyedsalehi, H. Kamani, J. Jaafari, A.H. Mahvi, Photocatalytic degradation of tetracycline using nanosized titanium dioxide in aqueous solution, Int. J. Environ. Sci. Technol., 12 (2015) 603–616.

[15] M. Bailón-Pérez, A. García-Campaña, C. Cruces-Blanco, M. del Olmo Iruela, Trace determination of β-lactam antibiotics in environmental aqueous samples using off-line and on-line preconcentration in capillary electrophoresis, J. Chromatogr. A, 1185 (2008) 273–280.

[16] K. Rahmani, M.A. Faramarzi, A.H. Mahvi, M. Gholami, A. Esrafili, H. Forootanfar, M. Farzadkia, Elimination and detoxification of sulfathiazole and sulfamethoxazole assisted by laccase immobilized on porous silica beads, Int. Biodeterior. Biodegrad., 97 (2015) 107–114.

[17] S. Behzadi, M. Dehghani, M. Sekhavatjoo, H. Hashemi, Optimization of Fenton process for total organic carbon removal from aqueous solution includes amoxicillin antibiotic by using Taguchi experimental design, J. Health. Syst. Res., 9 (2013) 1186–1200.

[18] H. Rahmani, M. Gholami, A.H. Mahvi, M. Ali-Mohammadi, K. Rahmani, Tinidazol antibiotic degradation in aqueous solution by zero valent iron nanoparticles and hydrogen peroxide in the presence of ultrasound radiation, J. Water. Chem. Technol., 36 (2014) 317–324.

[19] S.-F. Pan, M.-P. Zhu, J.P. Chen, Z.-H. Yuan, L.-B. Zhong, Y.-M. Zheng, Separation of tetracycline from wastewater using forward osmosis process with thin film composite membrane–Implications for antibiotics recovery, Sep. Purif. Technol., 153 (2015) 76–83.

[20] T.A. Gad-Allah, M.E.M. Ali, M.I. Badawy, Photocatalytic oxidation of ciprofloxacin under simulated sunlight, J. Hazard. Mater., 186 (2011) 751–755.

[21] A. Javid, S. Nasseri, A. Mesdaghinia, A.h. Mahvi, M. Alimohammadi, R.M. Aghdam, N. Rastkari, Performance of photocatalytic oxidation of tetracycline in aqueous solution by TiO_2 nanofibers, J. Environ. Health. Sci. Eng., 11 (2013) 1–6.

[22] E. Elmolla, M. Chaudhuri, Improvement of biodegradability of antibiotics wastewater by photo Fenton process, World. Appl. Sci. J., 5 (2008) 53–58.

[23] K.-J. Choi, S.-G. Kim, S.-H. Kim, Removal of antibiotics by coagulation and granular activated carbon filtration, J. Hazard. Mater., 151 (2008) 38–43.

[24] K.-J. Choi, H.-J. Son, S.-H. Kim, Ionic treatment for removal of sulfonamide and tetracycline classes of antibiotic, Sci. Total Environ., 387 (2007) 247–256.

[25] L.R. Rad, M. Irani, R. Barzegar, Adsorptive removal of acetaminophen and diclofenac using NaX nanozeolites synthesized by microwave method, Korean. J. Chem. Eng., 32 (2015) 1606–1612.

[26] S.D. Ashrafi, H. Kamani, J. Jaafari, A.H. Mahvi, Experimental design and response surface modeling for optimization of fluoroquinolone removal from aqueous solution by NaOH-modified rice husk, Desal. Water Treat., 57 (2016) 16456–16465.

[27] M.T. Samadi, R. Shokoohi, M. Araghchian, M. Tarlani Azar, Amoxicillin removal from aquatic solutions using multi-walled carbon nanotubes, J. Mazandaran. Univ. Med. Sci., 24 (2014) 103–115.

[28] H. Jafari Mansoorian, A.H. Mahvi, F. Kord Mostafapoor, M. Alizadeh, Equilibrium and synthetic studies of methylene blue dye removal using ash of walnut shell, J. Health. Field, 1 (2013) 48–55.

[29] R. Crisafully, M.A.L. Milhome, R.M. Cavalcante, E.R. Silveira, D. De Keukeleire, R.F. Nascimento, Removal of some polycyclic aromatic hydrocarbons from petrochemical wastewater using low-cost adsorbents of natural origin, Bioresour. Technol., 99 (2008) 4515–4519.

[30] M. Amin, A. Alazba, U. Manzoor, A review of removal of pollutants from water/wastewater using different types of nanomaterials, Adv. Mater. Sci. Eng., 2014 (2014) 1–24.

[31] H. Lu, J. Wang, M. Stoller, T. Wang, Y. Bao, H. Hao, An overview of nanomaterials for water and wastewater treatment, Adv. Mater. Sci. Eng., 2016 (2016) 1–10.

[32] X. Hou, J. Feng, X. Liu, Y. Ren, Z. Fan, M. Zhang, Magnetic and high rate adsorption properties of porous Mn1–xZnx-Fe$_2$O$_4$ (0≤x≤0.8) adsorbents, J. Colloid Interface Sci., 353 (2011) 524–529.

[33] B. Bapusaheb, T. Patil, Wastewater treatment using nanoparticles, J. Adv. Chem. Eng., 5 (2015) 1–2.

[34] K.M. Batoo, D. Salah, G. Kumar, A. Kumar, M. Singh, M.A. El-sadek, F.A. Mir, A. Imran, D.A. Jameel, Hyperfine interaction and tuning of magnetic anisotropy of Cu doped CoFe$_2$O$_4$ ferrite nanoparticles, J. Magn. Magn. Mater., 411 (2016) 91–97.

[35] J. Saffari, D. Ghanbari, N. Mir, K. Khandan-Barani, Sonochemical synthesis of CoFe$_2$O$_4$ nanoparticles and their application in magnetic polystyrene nanocomposites, J. Ind. Eng. Chem., 20 (2014) 4119–4123.

[36] M.H. Beyki, M. Shirkhodaie, F. Shemirani, Polyol route synthesis of a Fe$_3$O$_4$@CuS nanohybrid for fast preconcentration of gold ions, Anal. Methods, 8 (2016) 1351–1358.

[37] H.R. Pouretedal, N. Sadegh, Effective removal of Amoxicillin, Cephalexin, Tetracycline and Penicillin G from aqueous solutions using activated carbon nanoparticles prepared from vine wood, J. Water. Process. Eng., 1 (2014) 64–73.

[38] A. Norouzian Baghani, A.H. Mahvi, M. Gholami, N. Rastkari, M. Delikhoon, One-Pot synthesis, characterization and adsorption studies of amine-functionalized magnetite nanoparticles for removal of Cr (VI) and Ni (II) ions from aqueous solution: kinetic, isotherm and thermodynamic studies, J. Environ. Health. Sci. Eng., 14 (2016) 11.

[39] A.N. Baghani, A.H. Mahvi, N. Rastkari, M. Delikhoon, S.S. Hosseini, R. Sheikhi, Synthesis and characterization of amino-functionalized magnetic nanocomposite (Fe$_3$O$_4$–NH$_2$) for fluoride removal from aqueous solution, Desal. Water Treat., 65 (2017) 367–374.

[40] O. Moradi, A. Fakhri, S. Adami, S. Adami, Isotherm, thermodynamic, kinetics, and adsorption mechanism studies of Ethidium bromide by single-walled carbon nanotube and carboxylate group functionalized single-walled carbon nanotube, J. Colloid Interface Sci., 395 (2013) 224–229.

[41] K.Y. Foo, B.H. Hameed, Insights into the modeling of adsorption isotherm systems, Chem. Eng. J., 156 (2010) 2–10.

[42] X.-H. Li, C.-L. Xu, X.-H. Han, L. Qiao, T. Wang, F.-S. Li, Synthesis and magnetic properties of nearly monodisperse CoFe$_2$O$_4$ nanoparticles through a simple hydrothermal condition, Nanoscale. Res. Lett., 5 (2010) 1039–1044.

[43] Y. Huang, W. Wang, Q. Feng, F. Dong, Preparation of magnetic clinoptilolite/CoFe$_2$O$_4$ composites for removal of Sr^{2+} from aqueous solutions: Kinetic, equilibrium, and thermodynamic studies, J. Saudi Chem. Soc., 21 (2017) 58–66.

[44] S. Riyaz, A. Parveen, A. Azam, Microstructural and optical properties of CuS nanoparticles prepared by sol–gel route, Perspec. Sci., 8 (2016) 632–635.

[45] M.A. Gabal, S.S. Ata-Allah, Effect of diamagnetic substitution on the structural, electrical and magnetic properties of CoFe$_2$O$_4$, Mater. Chem. Phys., 85 (2004) 104–112.

[46] X. Li, W. Zhang, Y. Feng, W. Li, P. Peng, J. Yao, M. Li, C. Jiang, Ultrafine CoSe nano-crystallites confined in leaf-like N-doped carbon for long-cyclic and fast sodium ion storage, Electrochim. Acta, 294 (2019) 173–182.

[47] M.R. Samarghandi, T.J. Al-Musawi, A. Mohseni-Bandpi, M. Zarrabi, Adsorption of cephalexin from aqueous solution using natural zeolite and zeolite coated with manganese oxide nanoparticles, J. Mol. Liq., 211 (2015) 431–441.

[48] M. Ghaemi, G. Absalan, L. Sheikhian, Adsorption characteristics of Titan yellow and Congo red on CoFe$_2$O$_4$ magnetic nanoparticles, J. Iran. Chem. Soc., 11 (2014) 1759–1766.

[49] M.M. Hossain, J. Dean, Extraction of penicillin G from aqueous solutions: Analysis of reaction equilibrium and mass transfer, Sep. Purif. Technol., 62 (2008) 437–443.

[50] Z. Aksu, Ö. Tunç, Application of biosorption for penicillin G removal: comparison with activated carbon, Process Biochem., 40 (2005) 831–847.

[51] S. Moussavi, M. Ehrampoush, A. Mahvi, M. Ahmadian, S. Rahimi, Adsorption of humic acid from aqueous solution on single-walled carbon nanotubes, Asian J. Chem., 25 (2013) 5319–5324.

[52] S. Wu, X. Zhao, Y. Li, Q. Du, J. Sun, Y. Wang, X. Wang, Y. Xia, Z. Wang, L. Xia, Adsorption properties of doxorubicin hydrochloride onto graphene oxide: equilibrium, kinetic and thermodynamic studies, Materials, 6 (2013) 2026–2042.

[53] D. Balarak, F.K. Mostafapour, A. Joghataei, Experimental and kinetic studies on Penicillin G adsorption by Lemna minor, Br. J. Pharm. Res., 9 (2016) 1–10.

[54] S. Wu, X. Zhao, Y. Li, C. Zhao, Q. Du, J. Sun, Y. Wang, X. Peng, Y. Xia, Z. Wang, L. Xia, Adsorption of ciprofloxacin onto biocomposite fibers of graphene oxide/calcium alginate, Chem. Eng. J., 230 (2013) 389–395.

[55] D. Balarak, F.K. Mostafapour, H. Akbari, A. Joghtaei, Adsorption of amoxicillin antibiotic from pharmaceutical wastewater by activated carbon prepared from Azolla filiculoides, Br. J. Pharm. Res., 18 (2017) 1–13.

[56] C. Dong, W. Chen, C. Liu, Preparation of novel magnetic chitosan nanoparticle and its application for removal of humic acid from aqueous solution, Appl. Surf. Sci., 292 (2014) 1067–1076.

[57] S. Gueu, B. Yao, K. Adouby, G. Ado, Kinetics and thermodynamics study of lead adsorption on to activated carbons from coconut and seed hull of the palm tree, Int. J. Environ. Sci. Technol., 4 (2007) 11–17.

[58] K.Z. Elwakeel, Removal of Reactive Black 5 from aqueous solutions using magnetic chitosan resins, J. Hazard. Mater., 167 (2009) 383–392.

[59] S. Banerjee, M.C. Chattopadhyaya, Adsorption characteristics for the removal of a toxic dye, tartrazine from aqueous solutions by a low cost agricultural by-product, Arabian J. Chem., 10 (2017) S1629–S1638.

[60] A. Mahvi, A. Maleki, A. Eslami, Potential of rice husk and rice husk ash for phenol removal in aqueous systems, Am. J. Appl. Sci., 1 (2004) 321–326.

[61] A. Sheikh Mohammadi, M. Sardar, The removal of penicillin G from aqueous solutions using chestnut shell modified with H$_2$SO$_4$: Isotherm and kinetic study, Iran. J. Health. Environ., 5 (2013) 497–508.

[62] M. Malakootian, L. Ranandeh Kalankesh, Assessing the performance of silicon nanoparticles in adsorption of Humic acid in water, Iran. J. Health. Environ., 6 (2014) 535–544.

[63] H. Chen, J. Zhao, J. Wu, G. Dai, Isotherm, thermodynamic, kinetics and adsorption mechanism studies of methyl orange by surfactant modified silkworm exuviae, J. Hazard. Mater., 192 (2011) 246–254.

[64] B.H. Hameed, A.L. Ahmad, K.N.A. Latiff, Adsorption of basic dye (methylene blue) onto activated carbon prepared from rattan sawdust, Dyes Pigm., 75 (2007) 143–149.

[65] A. Dada, A. Olalekan, A. Olatunya, O. Dada, Langmuir, Freundlich, Temkin and Dubinin–Radushkevich isotherms studies of equilibrium sorption of Zn^{2+} unto phosphoric acid modified rice husk, IOSR J. Appl. Chem., 3 (2012) 38–45.

[66] H. Abdoallahzadeh, B. Alizadeh, R. Khosravi, M. Fazlzadeh, Efficiency of EDTA modified nanoclay in removal of humic acid from aquatic solutions, J. Mazandaran. Univ. Med. Sci., 26 (2016) 111–125.

[67] E. Bulut, M. Özacar, İ.A. Şengil, Adsorption of malachite green onto bentonite: equilibrium and kinetic studies and process design, Microporous Mesoporous Mater., 115 (2008) 234–246.

[68] A. Ziapour, Y. Hamzeh, A. Abyaz, Application of soybean waste as adsorbent of Acid Orange 7 from aqueous solution, J. Sep. Sci. Eng., 2 (2012) 29–38.

[69] Y.-S. Ho, Review of second-order models for adsorption systems, J. Hazard. Mater., 136 (2006) 681–689.